Quaternary Research 78 (2012) 323–332

Contents lists available at SciVerse ScienceDirect

Quaternary Research

journal homepage: www.elsevier.com/locate/yqres

The 1.5-ka varved record of Lake Montcortès (southern Pyrenees, NE Spain)

Juan Pablo Corella [a,b,*], Achim Brauer [c], Clara Mangili [c,g], Valentí Rull [d], Teresa Vegas-Vilarrúbia [e], Mario Morellón [a,f], Blas L. Valero-Garcés [a]

[a] Instituto Pirenaico de Ecología (IPE-CSIC), Avda Montañana 1005, 50059 Zaragoza, Spain
[b] Museo Nacional de Ciencias Naturales (MNCN-CSIC), Serrano 115bis, 28006 Madrid, Spain
[c] Deutsches GeoForschungsZentrum Potsdam, Sektion 5.2 Klimadynamik und Landschaftsentwicklung, D-14473 Potsdam, Germany
[d] Institut Botànic de Barcelona (IBB-CSIC-ICUB), Passeig del Migdia s/n, 08038 Barcelona, Spain
[e] Dept. Ecology, Fac. Biology. University of Barcelona, Avda Diagonal 643, 08028 Barcelona, Spain
[f] Eawag (Swiss Federal Institute of Aquatic Science & Technology), Überlandstrasse 133, 8600 Dübendorf, Switzerland
[g] Lamont–Doherty Earth Observatory, 61 Route 9W, PO Box 1000, Palisades, NY, USA

ARTICLE INFO

Article history:
Received 25 October 2011
Available online 5 July 2012

Keywords:
Biogenic varves
Human impact
Climate changes
Medieval Climate Anomaly
Little Ice Age
Pre-Pyrenees

ABSTRACT

The karstic Lake Montcortès sedimentary sequence spanning the last 1548 yr constitutes the first continuous, high-resolution, multi-proxy varved record in northern Spain. Sediments consist of biogenic varves composed of calcite, organic matter and detrital laminae and turbidite layers. Calcite layer thickness and internal sub-layering indicate changes in water temperature and seasonality whereas the frequency of detrital layers reflects rainfall variability. Higher temperatures occurred in Lake Montcortès in AD 555–738, 825–875, 1010–1322 and 1874–present. Lower temperatures and prolonged winter conditions were recorded in AD 1446–1598, 1663–1711 and 1759–1819. Extreme and multiple precipitation events dominated in AD 571–593, 848–922, 987–1086, 1168–1196, 1217–1249, 1444–1457, 1728–1741 and 1840–1875, indicating complex hydrological variability in NE Spain since AD 463. The sedimentary record of Lake Montcortès reveals a short-term relation between rainfall variability and the detrital influx, pronounced during extended periods of reduced anthropogenic influences. In pre-industrial times, during warm climate episodes, population and land use increased in the area. After the onset of the industrialization, the relationship between climate and human activities decoupled and population dynamics and landscape modifications were therefore mostly determined by socio-economic factors.

Introduction

High-resolution paleoenvironmental reconstructions are the key to understand climatic and human impact interactions for the last millennium. At a centennial scale, four main fluctuations characterized European climate during the last 1500 yr: i) the so-called Dark Ages Cold Period (DACP) (AD 450–900), documented as a cold phase in the Mediterranean Sea (Cini Castagnoli et al., 2002) and NW Iberia (Desprat et al., 2003); ii) the warm Medieval Climate Anomaly (MCA) (AD 900–1300) with relatively arid conditions in western Iberian Peninsula (IP) (Moreno et al., 2011, 2012); iii) colder and wetter conditions during the Little Ice Age (LIA) (AD 1300–1850) in the IP (Morellón et al., 2012; Fletcher and Zielhofer, in press); and iv) an increase in temperature during the last century (Mann and Bradley, 1999).

During the Holocene, human migrations and shifts in societies and economy have coincided with climate changes, suggesting a climate–human relationship. Nevertheless, paleoenvironmental reconstructions often lack the precise chronologies necessary to investigate the synchronicity and time lags of these climate–human interactions (Berglund, 2003). The eastern Sahara occupation during the Holocene Humid Period (Hoelzmann et al., 2001), and the Neolithic migrations that occurred in Europe (Turney and Brown, 2007) have been well-documented. In NE Spain, the cold 8.2 ka event has been considered responsible for regional human migrations (González-Sampériz et al., 2009). During the last millennium, large changes in European societies occurred synchronously with the MCA and the LIA (Zhang et al., 2007). In different regions of the IP, recent reconstructions show changes in land uses coinciding with significant shifts in the hydrology and vegetation during the MCA and the LIA (Martín-Puertas et al., 2008; Morellón et al., 2011; Rull et al., 2011). Currently, the Pre-Pyrenean Mountains are among the most depopulated regions in Europe. However, historical and documentary records indicate a higher population density during Medieval times and the late 19th century (Montserrat, 1992; García-Ruíz and Valero-Garcés, 1998; Riera et al., 2004; Fillat et al., 2008; Rull et al., 2011).

In this paper, we present a continuous 543-cm-long, varved, multi-proxy record from karstic Lake Montcortès (Pre-Pyrenees, NE Spain). Previous studies in this lake have demonstrated its millennial-to-

* Corresponding author at: Instituto Pirenaico de Ecología (IPE-CSIC), Avda Montañana 1005, 50059 Zaragoza, Spain. Fax: +34 915640800.
E-mail address: pablo.corella@mncn.csic.es (J.P. Corella).

0033-5894/$ – see front matter © 2012 University of Washington. Published by Elsevier Inc. All rights reserved.
doi:10.1016/j.yqres.2012.06.002

centennial sensitivity to climate variability during the middle and early Holocene (Corella et al., 2011; Scussolini et al., 2011) and the rapid response of vegetation to climate and human activities during the last millennium (Rull et al., 2011). This research constitutes the first annually resolved reconstruction of the last 1548 yr in the IP and thus provides a precise timing for the main climate fluctuations and land-use changes there.

Study area

Lake Montcortès is one of the few lakes in the Pre-Pyrenean Range (NE Spain) and one of the deepest karstic lakes in the IP (Alonso, 1998) (Fig. 1). The lake's watershed is situated in Triassic bedrock, mainly comprising carbonate, evaporite, claystone and shale formations (Rosell, 1994) (Fig. 1b). The lake is approximately circular, with a diameter of 1320 m and a maximum depth of 30 m. It is surrounded by steep talus (Camps et al., 1976; Corella et al., 2011; Fig. 1d).

The hydrology of Lake Montcortès is mainly controlled by groundwater and runoff as inputs and by evaporation and a small surface outlet as outputs. This emissary ravine in the northern shore (Figs. 1b, d) is a tributary of the Flamisell River, in the Ebro River Watershed, and controls the maximum water level of the lake. The lake is oligotrophic and meromictic, although short events of holomixis during winter have been documented (Modamio et al., 1988). A permanently anoxic monimolimnion occurs below 18–20 m water depth. Lake waters are of bicarbonate–sulfate–calcium type. Surface waters have an average pH of 8.4 and an electrical conductivity (EC) of 372 μS/cm, whereas in the anoxic hypolimnion, the pH is ca. 7.5 and the EC is ca. 528 μS/cm (Camps et al., 1976; Modamio et al., 1988; this study).

Lake Montcortès is located at the boundary between the Mediterranean lowlands and the Middle Montane belt, within the sub-Mediterranean bioclimatic domain (Rull et al., 2011), in a transitional climatic area with a strong rainfall gradient and, thus, is very sensitive to climate changes (Fig. 1a). Mean annual rainfall is 860 mm, and the most humid seasons are spring and autumn, with mean precipitations of 280 and 230 mm, respectively (Fig. 1c). Mean monthly temperature ranges from 1.9°C in the coldest month (January) to 20.3°C in the warmest (July) (Fig. 1c). Summer daily temperature variations can exceed 25°C, indicating the continental character of the regional Mediterranean alpine climate type.

Methods

Four cores from the deepest part of the lake were retrieved using a Kullenberg piston corer (Corella et al., 2011). All cores yielded a well-preserved varved record. The uppermost 528 cm of MON04-3A-1K core (Fig. 1d) was selected for this study due to the best preservation of the laminae and the absence of microfolding structures, which could have impeded accurate varve counting and microfacies characterization. The top sediments were analyzed in an additional gravity core (MON07-1A-1M). Therefore, a composite sequence of the uppermost 543 cm was sampled for large thin sections (100×15×35 mm), prepared using the freeze-dry technique and subsequent impregnation with epoxy resin (Araldite®) under vacuum conditions (Lotter and Lemcke, 1999; Brauer and Casanova, 2001). A Zeiss Axioplan 2 imaging optical microscope was used for microfacies studies and varve counting. In addition, ten sediment samples were studied with the scanning electron microscope (SEM) Ultra Plus Zeiss, coupled with an Edex (Baltec) analyzer (voltage 20 kV and analysis time of 30 s).

The elemental geochemical composition of core MON04-1A-1K was analyzed by X-ray fluorescence (XRF) using the ITRAX XRF core scanner from the Large Lakes Observatory (Duluth, University of Minnesota) with a 4-mm scanning resolution, 20 mA current, 30 s count time and 30 kV voltage. The results of XRF analyses of selected elements—phosphorus (P), iron (Fe), manganese (Mn) and titanium (Ti)—are expressed as element intensities in counts per second (cps). Stratigraphic correlations between cores were conducted through detailed smear-slide inspection. Detailed varve thickness measurements were performed with an optical microscope. A 50× magnification was used for layer measurements, except for the lower part of the record (543–540 cm), where varves were measured at 100× magnification due to their reduced thickness. The thicknesses of calcite, organic and occasional detrital layers were measured in each varve, except for the ones interpolated (5.1% of total varve number) due to poor preservation. Spearman correlation coefficients were calculated among the

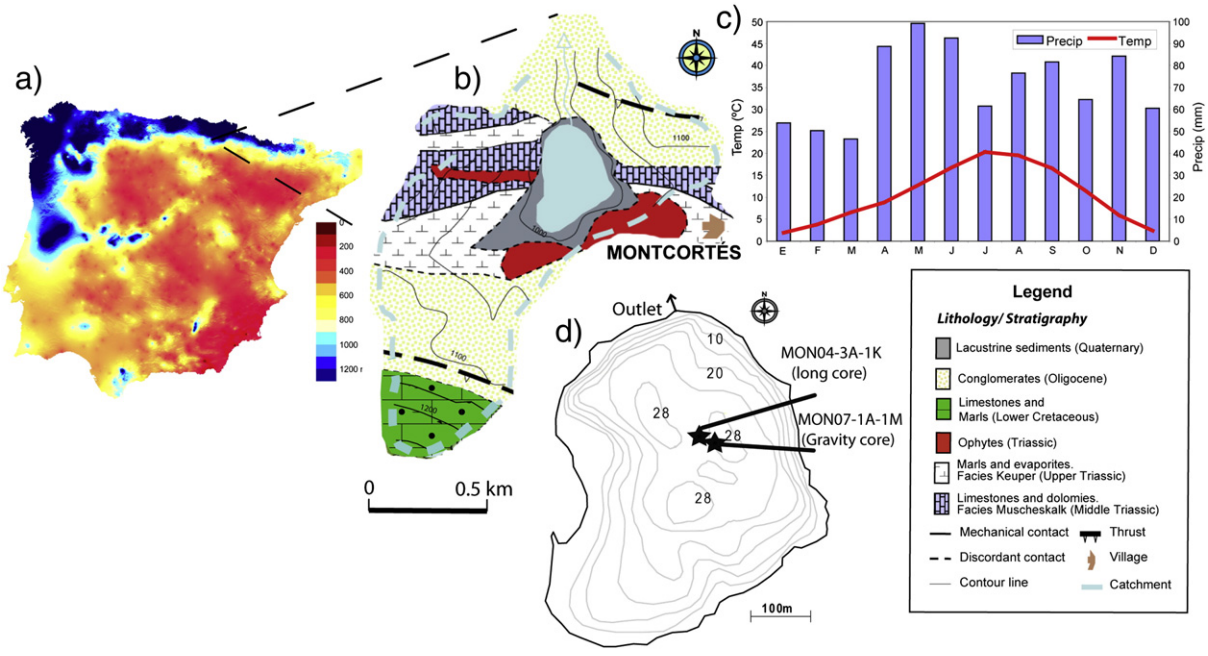

Figure 1. (a) Map of mean annual rainfall in the Iberian Peninsula (Ninyerola et al., 2005); (b) geological map of the Lake Montcortès catchment (42°19.50′N, 0°59.41′E; 1027 m a.s.l.); (c) ombrothermic diagram from Senterada Meteorological Station (5 km westward of the lake); and (d) Lake Montcortès bathymetric map and location of the retrieved sediment cores.

https://doi.org/10.1016/j.yqres.2012.06.002 Published online by Cambridge University Press

different variables of the data set with a statistical significance threshold of $p<0.01$. Sedimentological and geochemical variables were previously standardized. Varves were counted in selected 1-cm intervals based on the procedure described by Brauer and Casanova (2001). Standard error was estimated through double varve counting in selected intervals.

Results

Sedimentary microfacies

This study focuses on the uppermost 543 cm of the Lake Montcortès sedimentary sequence (Fig. 2a) spanning the last 1548 yr. It corresponds to the top four sedimentological units defined by Corella et al. (2011) composed of well-preserved varves punctuated by turbiditic layers. Two different microfacies (MF 1 and MF 2) have been identified within the Lake Montcortès varved sediments, depending on the presence of allocthonous detrital layers in the varve structure (Figs. 2b,c).

MF 1 corresponds to the classic biogenic varves described in lakes located in carbonate bedrock (Brauer, 2004), which are composed of a couplet of white, spring/summer, calcite and brownish, fall/winter, organic layers. On the other hand, MF 2 shows additional detrital layers (DL) between the calcite and organic laminae in the varve sequence.

The white calcite layer (Fig. 2b) is mainly composed of rhombohedric calcite crystals of variable sizes. The lower and upper boundaries of the calcite layer are sharp. Some diatoms, mainly *Cyclotella* specimens are included in the calcite layers. According to the texture of the calcite layer, in Lake Montcortès sediments, three main sub-layering types are observed (Fig. 2d): i) fining upward (coarse–fine, C–F) sequence, with a lower sub-layer of coarser calcite crystals (average size 12 μm) and an upper sub-layer of finer crystals (average size 5 μm), ii) coarsening upward (F–C), with a sub-layer of small crystals (average size 5 μm) followed by a layer of coarser crystals (average size 12 μm) and, iii) a homogeneous layer of coarse crystals (average size 12 μm). Although in some cases there is a gradual transition between the sub-layers, suggesting different settling velocities (Kelts and Hsü, 1978), most of the sub-layers show an abrupt boundary, indicating two distinct calcite precipitation pulses (Brauer et al., 2008).

The brownish organic matter-rich layer (Fig. 2b) is composed of amorphous organic matter, diatoms, detrital carbonate and quartz grains within a clayish matrix. *Cyclotella* spp. is the dominant diatom taxon, although pennate diatoms are also frequent. The presence of detrital material, particularly clay minerals, is highly variable, and reflects seasonal changes in sediment delivery to the lake, likely controlled by runoff and rainfall. This organic-rich layer is the result of deposition in Lake Montcortès after the period of calcite precipitation.

The grayish detrital layers (DL) (Fig. 2b) are composed of irregularly shaped detrital calcite, quartz and feldspar grains, terrestrial plant remains (bottom of the layer) and clay minerals, with a fining upwards texture. Dominant siliciclastic composition and sedimentary textures indicate that the layers were deposited by periods of increased runoff in the catchment.

According to the succession of the three layers in a varve (calcite, organic and DL), we distinguish two subtypes of MF 2. In microfacies MF 2a, the detrital layer occurs below or on top of the organic layer or even within the calcite layer indicating the season of deposition. In microfacies MF 2b there is a series of two to eight detrital layers on top of the calcite layer, in some occasions replacing the organic layer. MF 2b reflects an increase in frequency of the events delivering detrital sediments to the lake. The absence of a discrete organic layer in some varves could be due to: i) micro-erosion (Brauer et al., 2008), ii) dilution of the organic material within the detrital layers, iii) small irregularities in the lake floor, which may impede organic layer deposition in microtopographic reliefs or, iv) a decrease in organic productivity during those years caused by changes in limnological conditions such as increases in water turbidity linked to enhanced detrital input, and/or changes in nutrient input or temperature.

Turbidites include up to 12-cm-thick graded layers with erosional surfaces at the base (Fig. 2c). These turbidites show a discrete basal sub-layer of large, angular, sand-size quartz, rice-shaped calcite and gypsum crystals, abundant plant remains, and an upper sub-layer with higher amounts of clay minerals and amorphous organic matter. Some types of turbidites incorporate sub-angular calcite particles in the base, likely related to the reworking of littoral carbonated areas of the lake. In addition, some irregular and discontinuous gypsum-rich bands occur in the record, mainly within the turbidites strata. Gypsum crystals disrupt previous layers suggesting an early diagenetic origin of the gypsum.

Chronology

An independent varve chronology starting at AD 2007 has been established and complemented by four radiocarbon dates (Fig. 3) from plant and aquatic macrorests and bulk sediment samples obtained

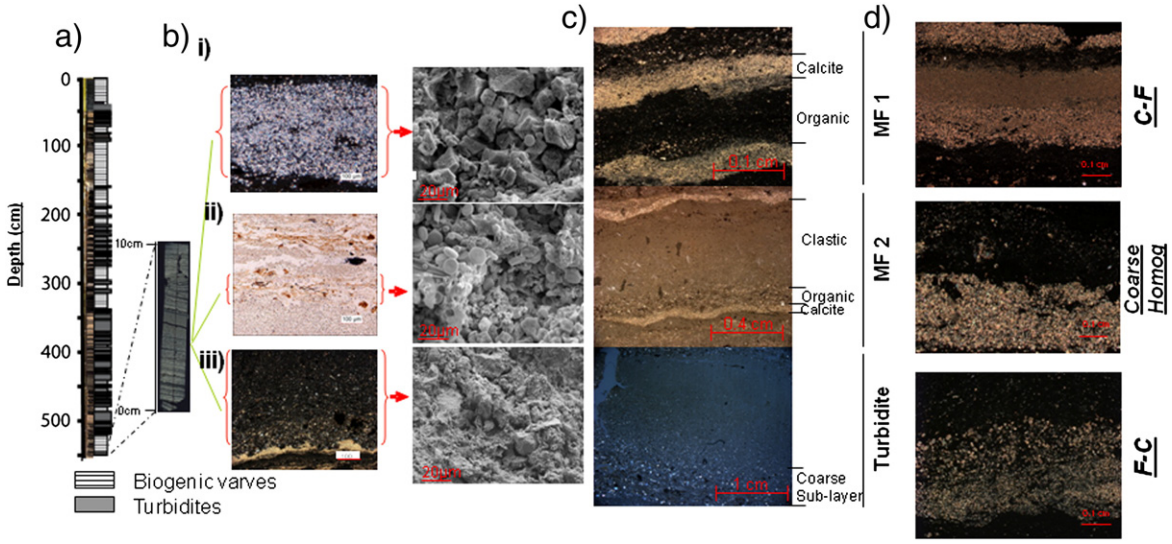

Figure 2. Biogenic varves from Lake Montcortès. (a) Stratigraphic column from MON04-3A-1K and MON07-1A-1M cores; (b) thin-section photos and SEM images of Montcortès varved sediments (MF 2): i) calcite layer; ii) organic layer and iii) detrital layer (DL); (c) microscopic images showing the two different varved micro-facies and a turbidite layer. (d) From top to bottom: coarse to fine (C–F), homogeneous coarse (Coarse Homog.) and fine to coarse (F–C) sub-layering succession examples of calcite layers.

https://doi.org/10.1016/j.yqres.2012.06.002 Published online by Cambridge University Press

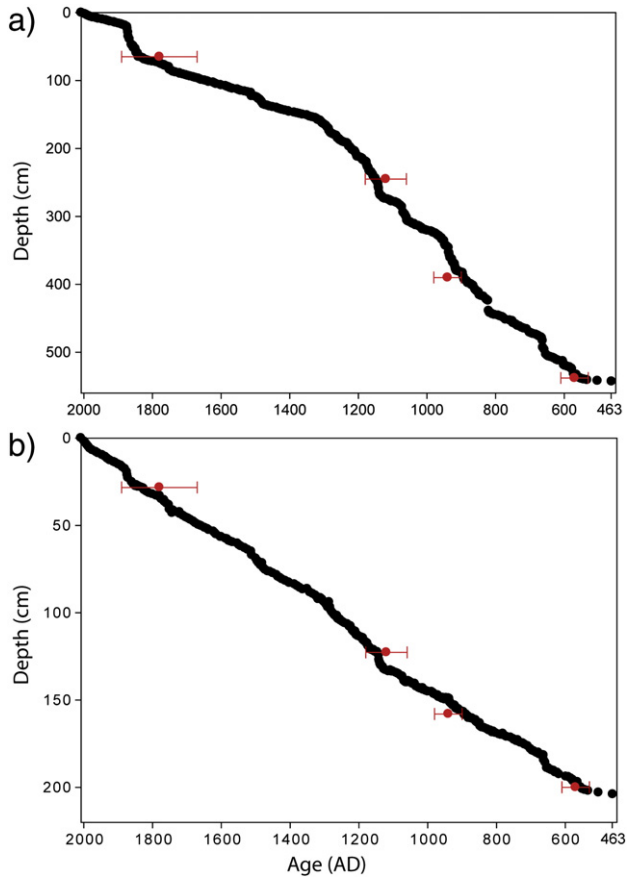

Figure 3. (a) Age–depth model for the last 1548 yr (varve yr AD) in the Lake Montcortès sedimentary sequence based on varve counting and AMS ^{14}C dates from Corella et al. (2011); and (b) corrected age–depth model after the extraction of the allocthonous input to the lake.

from the upper, middle and lower part of the studied interval, covering a time interval between AD 570–1780 (Corella et al., 2011). Since organic and detrital layers are not always present, each varve has been identified from the calcite layer. The good correlation of the varve counting with the ^{14}C AMS dates (Fig. 3) verifies the annual nature of the laminations.

From the total of 1548 varves, 79 of them, distributed in intervals of poor varve preservation (5.1%), have been interpolated using average sedimentation rates. Mean counting error oscillated between 0 and 3% depending on the varve quality and thus, represented a nonlinear error range throughout the sedimentary record. The average varve thickness or annual sedimentation rate (SR) fluctuates strongly, from 5 mm/yr between AD 533 and AD 1322 (540–182 cm depth) to 0.037 mm/yr between AD 463 and AD 533 (543–540 cm depth) (Fig. 3a). These changes in SR mainly reflect the variable detrital input; DL and turbidites represent 61.7% of the total thickness (543 cm) of the studied interval. If this clastic input is not included, the SR appears more constant (0.13 mm/yr), with the exception of the bottom 3 cm in the core, with a lower SR (0.037 mm/yr) (Fig. 3b).

Seasonal layer thickness, sedimentary textures and geochemistry

The large range of varve thickness, between less than 0.05 mm and 31.1 mm, indicates strongly fluctuating environmental conditions (Brauer and Casanova, 2001). Figure 4 shows the different seasonal layer thickness, sedimentary textures and XRF data distribution throughout the studied interval. A matrix showing correlation among the different proxies has been computed to explore the relationships within the dataset (Table 1).

Calcite and organic layers

Calcite and organic layer thicknesses largely oscillate from 0.04 up to 1.4 mm (calcite layers) and from 0.04 to 4 mm (organic layers) and show a weak correlation between them ($r = 0.38$, $p < 0.01$; Table 1). The periods AD 463–533, AD 680–1010 and AD 1322–1874 exhibit low calcite thicknesses (Table 2). In contrast, the periods AD 533–680, AD 1010–1322 and AD 1874–1992 show thicker calcite layers (Table 2).

Average calcite/organic lamina thickness ratios are relatively constant throughout the record (0.57), except for the AD 463–533 interval, when a high average ratio of 2.0 is characteristic. This high ratio is due to lower contents of detrital material in the organic layer. In general, most of the varves (87%) display homogeneous calcite layers, but different types of calcite sub-layering have been observed in particular intervals. Between AD 550 and AD 656, 43% of the varves exhibited a distinct coarse to fine (C–F) sub-layering. Since AD 656, the homogeneous coarse calcite layers became dominant whereas between AD 730 and AD 890, C–F sub-layers were observed only in 18% of the cases (Figs. 4 and 5). Varves with fine to coarse (F–C) sub-layering are present between AD 1322 and AD 1855 (19%). Highest percentages of F–C sub-layering are observed in the periods AD 1446–1598 (24%), AD 1663–1711 (35%) and AD 1759–1819 (28%). During the last century, both the C–F (8%) and F–C (10%) sub-layer types are present (Figs. 4 and 5).

Detrital layers and turbidites

The thickness of both detrital layers is highly variable, ranging from 0.1 mm to 11.2 mm (DL) and from 0.8 mm to 120 mm (turbidites) and strongly influence the varve thickness (Fig. 4; Table 1). Periods of thickest DL and turbidites reflect higher clastic input into the lake, with average DL and turbidite thicknesses of 1.16 and 6.8 mm, respectively (Table 3).

Geochemistry

The XRF downcore profiles of P and Ti in core 1A-1K show a coherent pattern with varve layer thickness variability (Fig. 4; Table 1). Ti displays higher values during the periods AD 665–972, 1020–1332 and 1844–1879, and frequently increases in clastic-dominated intervals, in which DL and turbidites are more abundant. Phosphorous increases during the intervals AD 660–1355 and AD 1843–1880, and it is also related to DL and turbidites throughout the sedimentary record. Finally, the Fe/Mn ratio displays higher values during AD 649–664, 970–1352 and 1842–1850.

Discussion

Paleoenvironmental proxies from varved records

Calcite layer thickness, calcite internal sub-layering, frequency and thickness of detrital layers and geochemical proxies (Ti, P and Fe/Mn ratio) reflect changes in water temperature, seasonality, trophic state of the lake, and erosion rates in the catchment of Lake Montcortès during the last 1548 yr (Figs. 4 and 5).

Geochemical proxies

The selected XRF data (Figs. 4 and 5) reflect biogeochemical relations in the lake and its catchment. Titanium is mostly delivered to the lake by oxides and silicates associated to the clay minerals entering the lake during periods of increased runoff. The Fe/Mn ratio also follows the detrital intervals but it does not exactly match the Ti curve (Fig. 4) because these elements are also dependent on changes in the redox conditions of the lake bottom and water column mixing evolution, with higher Fe/Mn ratio indicating anoxic hypolimnion and meromictic conditions in the lake (Schaller and Wehrli, 1996). Phosphorous cycle includes delivery from the catchment, storage in the sediments and release during anoxic conditions. Moderate correlation

https://doi.org/10.1016/j.yqres.2012.06.002 Published online by Cambridge University Press

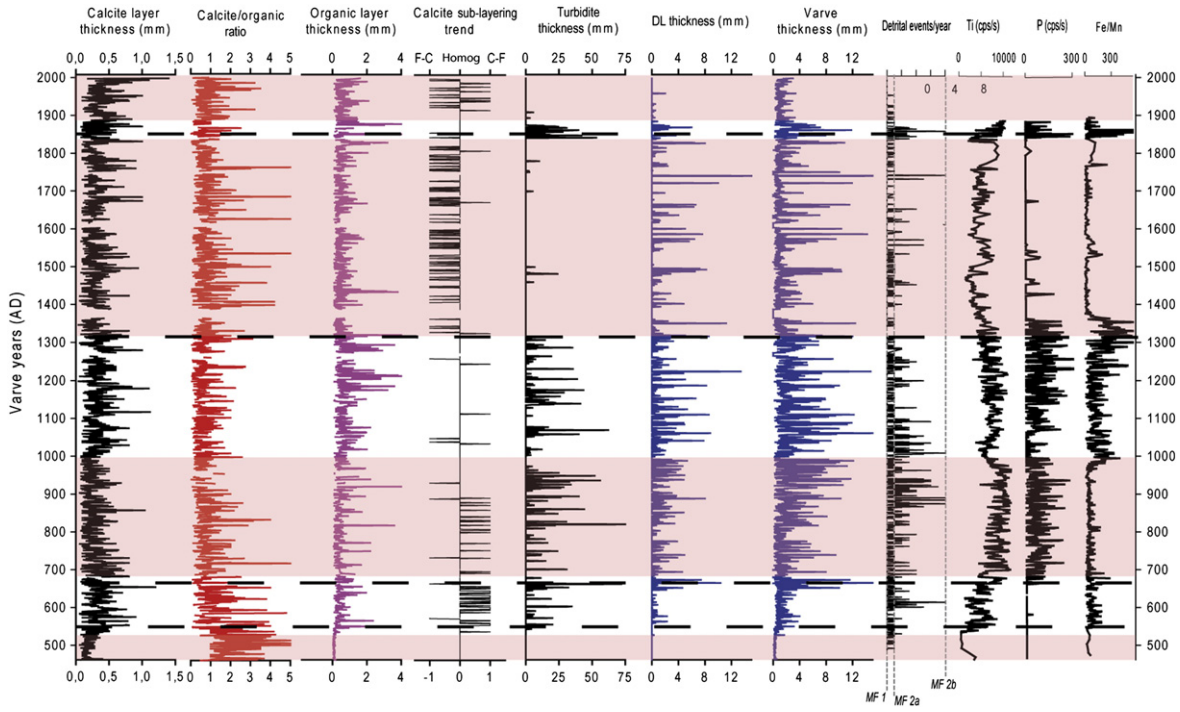

Figure 4. From left to right: calcite layer thicknesses and calcite sub-layering trends (F–C: fine to coarse sub-layering; Homog: homogeneous coarse calcite layer; F–C: coarse to fine sub-layering); DL and turbidite thicknesses; varve layer thicknesses; detrital events/yr; Ti, P, and Fe/Mn profiles (average resolution = 1.5 yr). Pink bands reflect the layer thickness changes for the intervals shown in Table 1. Dashed lines reflect the different periods observed in the calcite sub-layering.

between titanium and phosphorous ($r = 0.48$, $p < 0.01$; Table 1) could explain the influence of runoff on nutrient load to the lake and suggests an allocthonous source of the nutrients in the lake. Statistical relationships between phosphorous and Fe/Mn ratio ($r = 0.55$, $p < 0.01$; Table 1) also suggest how lake's eutrophication enhances stratification in the lake as a result of the strengthening of the oxic–anoxic boundary throughout the water column. The increase in the anoxic conditions in the lake bottom would have occurred during periods of higher nutrient load due to agricultural practices in the lake's catchment.

Calcite layer thickness

Calcite layers result from endogenic precipitation in the lake epilimnion related to calcite saturation enhanced by algal blooms (Brauer, 2004). Epilimnetic formation of calcite during spring/summer is typical in lakes emplaced in carbonate-rich bedrock areas (Zolitschka et al., 2003; Brauer et al., 2008) and hard-water lakes (Kelts and Hsü, 1978; Koschel, 1997; Romero-Viana et al., 2008). Mechanisms driving calcite precipitation are diverse, including several climatic and environmental forcings such as eutrophication, groundwater inflow and summer temperatures (Koschel, 1990; Brauer et al., 2008; Romero-Viana et al., 2008). In Lake Montcortès, no significant relationships between the phosphorous content in the sediment and the increase in the precipitation events per year, which ultimately control the groundwater regime, have been observed, suggesting that neither the nutrient availability nor groundwater inflow has a direct control on calcite precipitation in Lake Montcortès. On the other hand, thicker calcite layers during the warm MCA and thinner layers during the colder LIA suggest that temperature is the main driving factor on calcite precipitation in the lake.

Detrital layers and turbidite thickness and frequency

Detrital layers mainly result from deposition during runoff when clastic particles fall out of suspension during transportation to the lake during small flooding events, commonly leading to a local distribution

Table 1
Matrix correlation based on Spearman bilateral correlation of sedimentological and XRF proxy data in Lake Montcortès (calcite and organic, DL and turbidite layer thicknesses, calcite/organic, varve thickness and DL/yr, n = 1537; P, Fe/Mn and Ti, n = 1206).

	Calcite sub-layering	Organic layer thickness	Calcite/organic	Varve thickness	DL/yr	Turbidite thickness	DL thickness	P	Fe/Mn	Ti
Calcite layer thickness	0.03	**0.38**	**0.36**	**0.42**	0.05	**0.06**	0.02	0.00	0.00	0.01
Calcite sublayering		−0.04	−0.02	0.06	0.07	0.05	0.04	**0.15**	**0.25**	**0.13**
Organic layer thickness			−0.03	**0.35**	**−0.17**	**−0.10**	**−0.15**	−0.08	−0.08	−0.04
Calcite/organic				**−0.31**	**−0.31**	**−0.23**	**−0.25**	−0.03	−0.04	**−0.11**
Varve thickness					**0.77**	**0.32**	**0.72**	**0.10**	**0.06**	**0.14**
DL/yr						**0.50**	**0.85**	**0.14**	0.10	**0.16**
Turbidite thickness							**0.09**	**0.07**	0.06	**0.09**
DL thickness								**0.12**	0.08	**0.14**
P									**0.55**	**0.48**
Fe/Mn										**0.67**

Values significant at $p = < 0.01$ are in bold.

https://doi.org/10.1016/j.yqres.2012.06.002 Published online by Cambridge University Press

Table 2
Average layer thickness in Montcortès varves from identified sedimentary units.

Time periods (varve yr AD)	Calcite thickness (mm)	Organic thickness (mm)	Ratio Calcite/organic	Total varve thickness (mm)
463–533	0.18	0.09	2	0.28
533–680	0.35	0.47	0.74	1.53
680–1010	0.26	0.48	0.54	2.19
1010–1322	0.34	0.81	0.42	2.62
1322–1874	0.29	0.54	0.54	1.42
1874–1992	0.4	0.68	0.59	1.29

Table 3
Periods displaying maximum frequency and thickness of detrital layers and turbidites and average layer thickness.

		Years AD	Average thickness
Maximum thicknesses	DL	571–593, 754–834, 852–924, 968–1086, 1114–1158 1217–1255, 1421–1460, 1530–1565 and 1859–1874	1.16 mm
	Turbidites	571–593, 740–761, 845–888, 982–1011, 1069–1109 and 1842–1874	6.8 mm
Maximum frequency	MF 2b	571–593, 848–922, 987–1086, 1168–1196, 1217–1249 1444–1457, 1728–1741 and 1840–1875	

of the sediment load. The high frequency of MF 2b, characterized by more DLs per varve, represents multiple extreme precipitation events per year. On the other hand, the coarse basal layer and the erosional surface of turbiditic deposits likely result from underflow current processes, as result of inflowing water with higher density than lake water during large flood events and/or mass-movement processes (Sturm and Matter, 1978; Mulder and Alexander, 2001). The presence of reworked carbonate material is further evidence of erosion of the littoral platform during these events.

In the small catchment of Lake Montcortès, changes in land use could also strongly affect the detrital contribution to the lake. In fact, among the factors controlling the intensity of soil erosion, plant cover and land use are considered the most important, exceeding the influence of rainfall intensity and slope gradient (García-Ruiz, 2010). As discussed above, calcite layer thicknesses and calcite internal sub-layering are indicators of water temperature and changes in seasonality whereas DL/yr would indicate the frequency of precipitation events. On the other hand, DL and turbidite-layer thickness may respond to rainfall variability or land-use changes.

To fully evaluate the rainfall and temperature influence on the sediment delivery to the lake and their time lag response, two correlation matrices have been computed between the sedimentological proxies for two time intervals, the warm MCA, characterized by a strong anthropogenic pressure in Lake Montcortès catchment, and the LIA with a lower human impact in the area (Fig. 5; Table 4). No significant relationships between calcite layer thickness and turbidites and DL thicknesses were observed (Table 4), indicating a negligible short-term influence of temperature on the sediment availability in the catchment in different climatic and human-impact scenarios. On the other hand, strong correlation values between DL/yr and turbidite and DL thicknesses (Table 4) reveal the strong short-term impact of increase in rainfall frequency in the detrital contribution to the lake. A strong

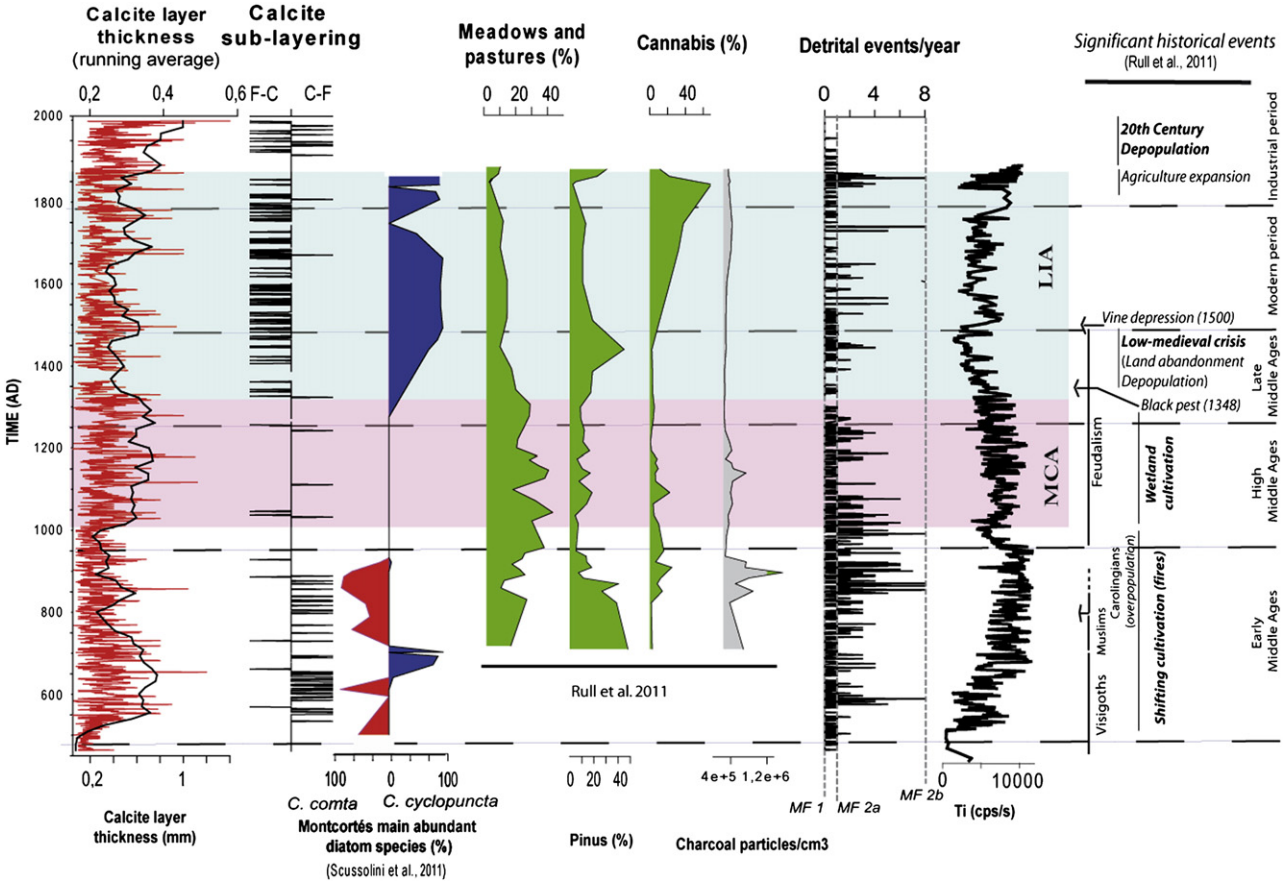

Figure 5. Comparison of calcite layer thicknesses and smoothed data (running average; sampling proportion = 0.03), different sub-layering types within calcite layers, frequency of detrital layers and detrital input (Ti profile) in the Lake Montcortès sedimentary sequence with pollen (Rull et al., 2011) and diatom (Scussolini et al., 2011) records from Lake Montcortès and main historical events in the area (Rull et al., 2011). Pollen resolution = 5–110 yr; diatom resolution = 2–165 yr.

https://doi.org/10.1016/j.yqres.2012.06.002 Published online by Cambridge University Press

Table 4
Matrix correlation of sedimentological proxy data in Lake Montcortès record for two time periods, MCA (AD 1010–1322) and LIA (AD 1322–1874).

MCA (n = 299)	Calcite layer thickness	Homog. coarse layers	DL/yr	Turbidite thickness	DL thickness
Calcite layer thickness	–	−0.01	0.04	0.07	0.01
Homog. coarse layers		–	−0.07	0.00	−0.08
DL/yr			–	**0.47**	**0.78**
Turbidite thickness				–	−0.02
DL thickness					–
LIA (n = 484)	**Calcite layer thickness**	**F–C sub-layering**	**DL/yr**	**Turbidite thickness**	**DL thickness**
Calcite layer thickness	–	**−0.26**	0.04	−0.02	0.05
F–C sublayering		–	0.12	0.09	0.10
DL/yr			–	**0.43**	**0.91**
Turbidite thickness				–	**0.12**
DL thickness					–

Values significant at $p = <0.01$ are in bold.

correlation value between DL/yr and DL thickness ($r = 0.91$; $p < 0.01$; Table 4) also highlights the direct influence of rainfall variability on the sediment input to the lake during periods of reduced anthropogenic influences. On the contrary, a lower correlation is shown during the MCA ($r = 0.78$; $p < 0.01$; Table 4). It suggests that persistent periods of higher human impact in the lake catchment may reduce the impact of rainfall frequency on the sediment supply to the lake at an annual scale. A long-term relationship between higher human impact and the increase of sediment supply into the lake is shown in Figure 5 suggesting that extended periods of higher land clearance and deforestation in the catchment also contribute to the sediment supply to the lake at a centennial to millennial scale.

Internal calcite sub-layering

Although factors controlling changes in the number and grain size of calcite sub-layers in varves are complex and not well-understood yet, variations in sub-layer successions appear to correspond to environmental factors including temperature, water composition, and the presence of phosphorous (Brauer et al., 2008). Biological differences in the species of diatoms involved produce additional differences in calcite sub-layering fluctuations (Stabel and Chondrogianni, 1988). Consequently, calcite sub-layering in Lake Montcortès apparently responds to water temperature, the trophic state of the lake, and the timing of the different diatom blooms. Diatom species accounting for main plankton blooms in Lake Montcortès, *Cyclotella comta* and *Cyclotella cyclopuncta*, display different autoecological trends and occurred in different intervals of the diatom record (Scussolini et al., 2011). The coincidence of each of these species with different sub-layering types (C–F and F–C) (Fig. 5) suggests a link between the nucleation of calcite crystals and the timing of the diatom bloom.

In Lake Montcortès, the C–F sub-layering may be interpreted as the result of calcite precipitation during warmer periods. The C–F texture coincides with the presence of *C. comta* in the record. This diatom species is resistant to high water temperatures (Thomas and Gonzalves, 1965) and has been reported to bloom in spring and summer during thermal stratification (Dorgelo et al., 1981; Anneville et al., 2002). The coarse sub-layer may precipitate when waters are not supersaturated in calcite during prolonged spring warming, with the subsequent nucleation of larger crystals. Warmer temperatures during summer likely favor blooms of *C. comta* enhancing calcite supersaturation leading to the fine-grained sub-layer precipitation, due to a rapid nucleation and production of smaller calcite crystals. The C–F sub-layering also has been interpreted as a succession of two different production pulses in other lakes (Geyh et al., 1971; Kelts and Hsü, 1978; Brauer et al., 2008).

The F–C sub-layering may be related to changes in seasonality involving lower water temperatures due to prolonged winter conditions and a delayed warming in spring. Such conditions may have caused an immediate supersaturation leading to rapid nucleation of small calcite crystals (Folk, 1974; Brauer et al., 2008). The F–C texture coincides with *C. cyclopuncta*, which prefers oligotrophic to mesotrophic water (Finsinger et al., 2006; Tolotti et al., 2007; Kirilova et al., 2010). It thrives mainly during spring (Anneville et al., 2002; Padisak et al., 2003) and has also been recorded in Southern Alps lakes during the last phases of the LIA (Finsinger et al., 2006; Bigler et al., 2007). Based on these facts, we assume that *C. cyclopuncta* peaks in colder waters. Besides a delayed spring warming, the F–C texture might also be related to the bloom of *C. cyclopuncta*, which might produce excess nuclei for crystal formation and deposition of the fine-grained sub-layer. The decrease of this dominant diatom species after the main spring bloom would decrease calcite supersaturation, contributing to slower nucleation and formation of larger crystals.

The homogeneous coarse layers possibly respond to changes in the nutrient input to the lake, as reflected by the phosphorous content in the sediment. The anoxic bottom conditions in Lake Montcortès, indicated by higher Fe/Mn ratio (Fig. 4), would contribute to the release of phosphorous from bottom sediments to anoxic bottom waters. Occasional mixing events, as the one described by Modamio et al. (1988) would bring large amounts of phosphorous to the photic zone where calcite precipitates (Burley et al., 2001). Dissolved phosphorous would lead to a decrease in the calcite crystal nucleation density (House, 1987) and a subsequent formation of these larger, homogeneous-sized crystals (Stabel and Chondrogianni, 1988). Homogeneous coarse calcite crystal layers were abundant between AD 656–1400 and AD 1855–1913, coinciding with documented periods of increasing farming activities during the Middle Ages and the 19th century (Fig. 4).

Climate and human synergies

Previous studies of the Montcortès sequence have shown millennial- and centennial-scale Holocene hydrological and limnological fluctuations based on a ^{14}C AMS chronological framework (Corella et al., 2011; Rull et al., 2011; Scussolini et al., 2011). Corella et al. (2011) reconstructed the different depositional environments in the lake during the last 6000 yr and evaluated the triggering mechanisms influencing the sediment delivery to the lake, with an abrupt increase during the last 1200 yr. A paleoecological reconstruction carried out by Scussolini et al. (2011) revealed strong fluctuations in diatom species assemblage compositions suggesting arid conditions and intense anthropogenic pressure in the lake catchment during the MCA and an increase in the effective moisture during the LIA. Rull et al. (2011) performed a detailed reconstruction of the vegetation dynamics during the last 1200 yr. These palynological analyses provide evidence of the influence of both climate and human impacts

https://doi.org/10.1016/j.yqres.2012.06.002 Published online by Cambridge University Press

modulating the landscape during the last millennium. Fluctuations of a low Mediterranean scrub community indicated a warm MCA and a progressive cooling during onset of the LIA in the 15th century that coincided with a decline of human activities in the area.

The varve chronology and micro-facies analyses shown in this study allow a more detailed reconstruction of climate, lake dynamics, and land-use changes during the last 1548 yr, allowing the identification of five main stages.

The end of the Roman Period and Early Middle Ages (5th–8th centuries)

The increase in calcite layer thickness during the periods AD 555–738 and AD 825–875 and the more frequent occurrence of the coarse to fine (C–F) calcite sub-layering (43% of the varves in the interval) since AD 550 are likely related to higher water temperatures during those periods. The reduction of the C–F sub-layering frequency between AD 656 and 890 (18%) coincides with an abrupt increase in the phosphorous content in the sedimentary record since AD 656 (Fig. 4) due to a higher trophic state of the lake; this, in turn, may control the presence of the coarse calcite crystals in homogeneous layers and the absence of sub-layering. An increase in DL/yr between AD 571 and AD 593 indicates more rainfall events during this period.

The end of the Roman Period is also characterized by low clastic input and thus, reduced erosion in the lake watershed. Since AD 533, the onset of frequent MF 2 and turbidites reveals an abrupt change and higher runoff in the lake catchment due to a decrease in the vegetation cover as a consequence of shifting cultivation in the area (Fig. 5; Rull et al., 2011).

The High Middle Ages (9th–14th centuries)

Warmer conditions during the MCA are indicated in Lake Montcortès record by thicker calcite layers between AD 1010 and AD 1322 and, particularly since AD 1119. The highest rainfall frequency of the last 1548 yr occurred between AD 848 and AD 922, as indicated by the increase in frequency of DL/yr and thicker DL (Fig. 5). Extreme and multiple precipitation events as indicated by MF 2b also dominated during the periods AD 987–1086, 1168–1196 and 1217–1249. The paleoclimatic reconstruction in Lake Montcortès during this period is in agreement with other marine and lacustrine sequences in the IP that show warm and arid conditions during the MCA (Moreno et al., 2011; Morellón et al., 2012; Moreno et al., 2012). Nevertheless, the high-resolution paleohydrological record in Lake Montcortès underlines a complex hydrological variability in NE Spain during the MCA.

The highest clastic input in Lake Montcortès started at AD 852 and lasted for about five centuries, indicative of an increase in human activities around the lake, which is also reflected by an increase in the extension of pastures at the expense of pine forest, especially since the 9th century (Fig. 5, Rull et al., 2011). Thicker DL during the periods AD 852–924, 968–1086, 1114–1158 and 1217–1255, may be related to a combination of more intense land use and an increase in surface runoff events. The interval AD 852–924 is further characterized by higher frequency of fire events in the lake watershed, as shown by charcoal peaks between AD 862 and 933 (Fig. 5). Two periods of higher runoff coincide with periods of meadows and pasture development in the catchment during AD 959–1044 and 1124–1179. The increase in Fe/Mn between AD 950 and 1360 indicates more anoxic conditions in the lake hypolimnion while the persistence of larger calcite crystals during this same period may reflect a high trophic state of the lake due to intensive land use. This increase in the anthropogenic activities during the High Middle Ages may have also been enhanced by the favorable climate conditions in this mid-mountain area during the warm MCA.

The Little Ice Age (LIA, 14th–18th centuries)

The absence of turbidites and the significant decrease in MF 2 since AD 1322 (Fig. 5) reflect an abrupt decrease in the sediment delivery to the lake that occurred synchronously with the onset of the LIA. Colder temperatures and prolonged winter conditions occurred in the Lake Montcortès during the LIA as indicated by a decrease in the calcite layer thickness (Table 2) and the onset of the fine to coarse (F–C) calcite sublayering between AD 1322 and 1855. This sub-layering was particularly frequent during AD 1446–1598, AD 1663–1711 and AD 1759–1819 (Fig. 5), indicating the coldest intervals of the LIA in the area. An increase in the rainfall frequency was recorded during AD 1444–1457 and AD 1728–1741. Interestingly, the second episode correlates with a period of large floods in the nearby Segre River (Rico, 2004). The Lake Montcortès record is coherent with most of the paleoclimatic records in western Mediterranean that suggest prevailing cold and generally wet conditions during the LIA (Fletcher and Zielhofer, in press). In addition, this varved record provides a precise timing and extension of the different phases of the LIA and highlights a higher hydroclimate heterogeneity of this cooling phase in NE Spain, in agreement with Morellón et al. (2012).

Less favorable climatic conditions during this period may also have caused a reduction in settlement density in the area, as indicated by the significant decrease in meadows and pastures, and the increase in pine forests (Rull et al., 2011; Fig. 5). A well-documented depopulation during the mid 14th century (Marugan and Oliver, 2005) related to numerous internal wars during the Low-Medieval crisis and the Black Death pandemic, caused an abrupt decrease in farming activities. The decrease in population is reflected by reduced erosion in the catchments, as supported by the absence of turbidites and a decrease in Ti and DL thickness (Figs. 4 and 5). Human impact in the lake's catchment remained low during the LIA, as indicated by low pastures and charcoal values and the reduced clastic input to the lake, Nevertheless, *Cannabis* increased progressively from the 16th century. The *Cannabis* increase indicates that hemp retting had already started, likely as a consequence of the naval industry demand for hemp fiber (Rull et al., 2011).

The end of the LIA and the 20th century

An abrupt increase in detrital input (MF 2 and turbidites) to the lake occurred during the 19th century. More abundant flood layers (MF 2b) between AD 1842 and 1874 reflect the observed increase in the frequency and severity of floods in NE Spain (Rico, 2004; Llasat et al., 2005). Interestingly, this period is synchronous with the last cold spells of the LIA in this region (Morellón et al., 2011) and to the highest demographic pressure in most mountain valleys of the Spanish Pyrenees between AD 1840 and 1860 (Ayuda and Pinilla, 2002; Fillat et al., 2008). During that time, slash-and-burn was a common practice and marginal steep slopes were cultivated even under shifting agriculture systems without any special conservation measures (Lasanta, 1989). Furthermore, the detrital input increase coincides with the period of higher *Cannabis* production and hemp retting during the 19th century (Rull et al., 2011) (Fig. 5), which has been also observed in other nearby lacustrine records as, for example, Lake Estanya (Riera et al., 2004). The hemp retting was likely carried out directly in the lake or around it, affecting the littoral vegetation, thus favoring higher clastic input to the lake (Fig. 5).

The decline of the clastic input and higher calcite precipitation after AD 1874 and during the 20th century is likely due to changes in the economy of this mountain area. The Pallars population decreased between AD 1870 and 1910 (Farràs, 2005), as a consequence of industrialization and agricultural crisis. Massive emigration from rural zones to urban areas occurred during the 20th century and, in particular, after the 1950s reduced the human pressure on the environment (García-Ruiz, 2010).

During the last two centuries, the relation between climate and human activities in the area, also indicated in the nearby Lake Estanya record with a parallel evolution of cultivated taxa and mesothermophytes during moister and warmer conditions (Morellón et al., 2011), became increasingly decoupled. Thus, the intense land use and population expansion in the area during the last cold phases of the LIA, with harsh

https://doi.org/10.1016/j.yqres.2012.06.002 Published online by Cambridge University Press

climate for human activities in this area, contrast with the depopulation of the area during the warmer 20th century.

Conclusions

The sedimentary record of Lake Montcortès consists of a continuous sequence of biogenic varves punctuated by detrital layers. Different microfacies types and features, including calcite layer thickness variations and sub-layering, frequency and thickness of detrital layers, reflect variable patterns of climate change and landscape occupation since Medieval Ages until recent times. The lacustrine stratigraphic record indicates that warmer conditions occurred during the periods AD 555–738, 825–875, 1010–1322 and 1874–present day, while the coldest periods correspond to AD 1446–1598, 1663–1711 and 1759–1819. Estimates of higher rainfall frequency during AD 571–593, 848–922, 987–1086, 1168–1196, 1217–1249, 1444–1457, 1728–1741 and 1840–1875 suggest a complex paleohydrological structure during the last 1548 yr. Warmer conditions during the MCA (AD 1010–1322) and cold during the LIA (AD 1322–1874) are coherent with most paleoclimatic reconstructions in NE Iberian Peninsula. In addition, this varved record allows a further comprehension of the timing and extension of the main climatic phases and hydrological variability during the last millenium in NE Spain in comparison with other marine and lacustrine sequences based on ^{14}C AMS chronological framework.

The varved Lake Montcortès record suggests a complex, two-fold history of changing climate–human synergies during the last 1548 yr, rather than control by climate or human land use, as sometimes assumed for Mediterranean mountain landscape evolution. During the pre-industrial period, a strong link between climate and human activities in the catchment is evident. Population increased during the Late Middle Ages under warmer climate conditions (MCA) and caused a higher sediment delivery and nutrient loading into the lake, leading to an increase in trophic conditions. Colder climate during the onset of the LIA coincided with a decrease in human activities since AD 1322. This distinct link between climate and human occupation in the area is not observed in the post-LIA period when anthropogenic activities decreased despite a warmer and more favorable climate.

Acknowledgments

Financial support for this research was provided by the Spanish Inter-Ministry of Science and Technology (CICYT), through the projects GLOBALKARST (REN2003-09130-C02-02), and GRACCIE (CSD2007-00067). Additional funding was provided by the Aragonese Regional Government-CAJA INMACULADA and a bilateral DAAD-CICYT project, which partially funded microfacies analysis at GFZ (Potsdam) through a travel grant. Juan Pablo Corella was supported by a PhD contract with CONAI + D (Aragonese Scientific Council for Research and Development), Mario Morellón is supported by a postdoctoral fellowship funded by the Spanish Ministry of Education and Science and Clara Mangili hold postdoctoral a fellowship at Lamont–Doherty Earth Observatory, respectively. We thank Arsenio Muñoz for his comments and suggestions in this paper. We are also indebted to the GFZ and IPE-CSIC laboratory staffs for their collaboration in this research. The comments of J.C. Knox, Santiago Giralt and of an anonymous reviewer greatly improved a previous version of the manuscript.

References

Alonso, M., 1998. Las lagunas de la España peninsular. Limnética 15, 1–176.
Anneville, O., Ginot, V., Angeli, N., 2002. Restoration of Lake Geneva: expected versus observed responses of phytoplankton to decreases in phosphorus. Lakes and Reservoirs: Research and Management 7, 67–80.
Ayuda, M.A., Pinilla, V., 2002. El proceso de desertización demográfica de la montaña pirenaica en el largo plazo. Ager 2, 101–138.
Berglund, B., 2003. Human impact and climate changes—synchronous events and a causal link? Quaternary International 105, 7–12.
Bigler, C., von Gunten, L., Lotter, A.F., Hausmann, S., Blas, A., Ohlendorf, C., Sturm, M., 2007. Quantifying human-induced eutrophication in Swiss mountain lakes since AD 1800 using diatoms. The Holocene 17, 1141–1154.
Brauer, A., 2004. Annually laminated lake sediments and their palaeoclimatic relevance. In: Fischer, H., Kumke, T., Lohmann, G., Flöser, G., Miller, G., von Storch, H., Negendank, J.F.W. (Eds.), The Climate in Historical Times. Towards a Synthesis of Holocene Proxy Data and Climate Models. Springer, Berlin, pp. 109–128.
Brauer, A., Casanova, J., 2001. Chronology and depositional processes of the laminated sediment record from Lac d'Annecy, French Alps. Journal of Paleolimnology 25, 163–177.
Brauer, A., Mangili, C., Moscariello, A., Witt, A., 2008. Palaeoclimatic implications from micro-facies data of a 5900 varve time series from the Piànico interglacial sediment record, southern Alps. Palaeogeography, Palaeoclimatology, Palaeoecology 259, 121–135.
Burley, K.L., Prepas, E.E., Chambers, P.A., 2001. Phosphorus release from sediments in hardwater eutrophic lakes: the effects of redox-sensitive and -insensitive chemical treatments. Freshwater Biology 46, 1061–1074.
Camps, J., Gonzalvo, I., Güell, J., López, P., Tejero, A., Toldrà, X., Vallespinos, F., Vicens, M., 1976. El lago de Montcortès, descripción de un ciclo anual. Oecología acuática 2, 99–110.
Cini Castagnoli, G., Bonino, G., Taricco, C., Bernasconi, S.M., 2002. Solar radiation variability in the last 1400 years recorded in the carbon isotope ratio of a Mediterranean Sea core. Advances in Space Research 29, 1987–1994.
Corella, J.P., Moreno, A., Morellón, M., Rull, V., Giralt, S., Rico, M., Pérez-Sanz, A., Valero-Garcés, B.L., 2011. Climate and human impact on a meromictic lake during the last 6,000 years (Montcortès Lake, Central Pyrenees, Spain). Journal of Paleolimnology 46, 351–367.
Desprat, S., Sánchez Goñi, M.F., Loutre, M.F., 2003. Revealing climatic variability of the last three millennia in northwestern Iberia using pollen influx data. Earth and Planetary Science Letters 213, 63–78.
Dorgelo, J., Van Donk, E., De Graaf Bierbrauwer, I.M., 1981. The late winter/spring bloom and succession of diatoms during four years in lake Maarsseveen (The Nertherlands). Verhandlungen der Internationalen Vereinigung für Limnologie 21, 938–947.
Farràs, F., 2005. El Pallars contemporani. In: Marugan, C.M., Rapalino, V. (Eds.), Història del Pallars. Dels orígens als nostre dies. Pagès Editors, Lleida, pp. 121–144.
Fillat, F., García-González, R., Gómez, D., Reiné, R., 2008. Pastos del Pirineo. Consejo Superior de Investigaciones Científicas (C.S.I.C.), Madrid.
Finsinger, W., Bigler, C., Krähenbüh, U., Lotter, A.F., Ammann, B., 2006. Human impacts and eutrophication patterns during the past 200 years at Lago Grande di Avigliana (N. Italy). Journal of Paleolimnology 36, 55–67.
Fletcher, W.J., Zielhofer, C., in press. Fragility of western Mediterranean landscapes during Holocene rapid climate changes. Catena, http://dx.doi.org/10.1016/j.catena.2011.05.001.
Folk, R.L., 1974. The natural history of crystalline calcium carbonate; effect of magnesium content and salinity. Journal of Sedimentary Petrology 44, 40–53.
García-Ruiz, J.M., 2010. The effects of land uses on soil erosion in Spain: a review. Catena 81, 1–11.
García-Ruíz, J.M., Valero-Garcés, B.L., 1998. Historical geomorphic processes and human activities in the Central Spanish Pyrenees. Mountain Research and Development 18, 309–320.
Geyh, M.A., Merkt, J., Müller, H., 1971. Sediment pollen und Isotopenanalysen an jahreszeitlich geschichiteten Ablagerungen im zentralen Teil des Schleinsees. Archiv für Hydrobiologie 69, 366–399.
González-Sampériz, P., Utrilla, P., Mazo, C., Valero-Garcés, B.L., Sopena, M.C., Morellón, M., Sebastián, M., Moreno, A., Martínez-Bea, M., 2009. Patterns of human occupation during the early Holocene in the Central Ebro Basin (NE Spain) in response to the 8.2 ka climatic event. Quaternary Research 71, 121–132.
Hoelzmann, P., Keding, B., Berker, H., Krípelin, S., Kruse, H.J., 2001. Environmental change and archaeology: lake evolution and human occupation in the eastern Sahara during the Holocene. Palaeogeography, Palaeoclimatology, Palaeoecology 169, 193–217.
House, W.A., 1987. Inhibitation of calcite crystals growth by inorganic phosphate. Journal of Colloid and Interface Science 119, 505–511.
Kelts, K., Hsü, K.J., 1978. Freshwater carbonate sedimentation. In: Lerman, A. (Ed.), Lakes: Chemistry, Geology, Physics. Springer, New York, pp. 295–323.
Kirilova, E.P., Cremer, H., Heiri, O., Lotter, A.F., 2010. Eutrophication of moderately deep Dutch lakes during the past century: flaws in the expectations of water management? Hydrobiologia 637, 157–171.
Koschel, R., 1990. Pelagic calcite precipitation and trophic state of hardwater lakes. Archiv für Hydrobiologie-Beiheft Ergebnisse der Limnologie 33, 380–408.
Koschel, R., 1997. Structure and function of pelagic calcite precipitation in lake ecosystems. Verhandlungen der Internationalen Vereinigung für Limnologie 26, 343–349.
Lasanta, T., 1989. Evolución reciente de la agricultura de montaña: El Pirineo aragonés. Geoforma, Logroño.
Llasat, M.C., Rigo, T., Barriendos, M., 2005. Floods in Catalonia (NE Spain) since the 14th century. Climatologial and meteorological aspects from historical documentary sources and old instrumental records. Journal of Hydrology 313, 32–47.
Lotter, A.F., Lemcke, G., 1999. Methods for preparing and counting biochemical varves. Boreas 28, 243–252.
Mann, M.E., Bradley, R.S., 1999. Northern Hemisphere temperatures during the past millenium: inferences, uncertainties, and limitations. Geophysical Research Letters 26, 759–762.
Martín-Puertas, C., Valero-Garcés, B.L., Mata, P., González-Sampériz, P., Bao, R., Moreno, A., Stefanova, V., 2008. Arid and humid phases in southern Spain during the last 4000 years: the Zoñar Lake Record, Córdoba. The Holocene 18, 907–921.

Marugan, C.M., Oliver, J., 2005. El Pallars Medieval. In: Marugan, C.M., Rapalino, V. (Eds.), Història del Pallars. Dels orígens als nostre dies. Pagès Editors, Lleida, pp. 45–86.
Modamio, X., Pérez, V., Samarra, F., 1988. Limnología del lago de Montcortès (ciclo 1978–79) (Pallars Jussà, Lleida). Oecología Aquática 9, 9–17.
Montserrat, J., 1992. Evolución glaciar y postglaciar del clima y la vegetación en la vertiente sur del Pirineo: estudio palinológico. Consejo Superior de Investigaciones Científicas (C.S.I.C.), Madrid.
Morellón, M., Valero-Garcés, B.L., González-Sampériz, P., Vegas-Vilarrúbia, T., Rubio, E., Rieradevall, M., Delgado-Huertas, A., Mata, P., Romero, Ó., Engstrom, D., López-Vicente, M., Navas, A., Soto, J., 2011. Climate changes and human activities recorded in the sediments of Lake Estanya (NE Spain) during the Medieval Warm Period and Little Ice Age. Journal of Paleolimnology 46, 423–452.
Morellón, M., Pérez-Sanz, A., Corella, J.P., Büntgen, U., Catalán, J., González Sampériz, P., González-Trueba, J.J., López-Sáez, J.A., Moreno, A., Pla, S., Saz Sánchez, M.Á., Scussolini, P., Serrano, E., Steinhilber, F., Stefanova, V., Vegas Vilarrúbia, T., Valero-Garcés, B., 2012. A multi-proxy perspective on millennium-long climate variability in the Southern Pyrenees. Climate of the Past Discussions 8, 683–700.
Moreno, A., Morellón, M., Martín-Puertas, C., Frigola, J., Canals, M., Cacho, I., Corella, J.P., Pérez, A., Belmonte, A., González-Sampériz, P., Valero-Garcés, B.L., 2011. Moisture fluctuations reconstructed from paleoclimate archives in the Iberian Peninsula: is there a common pattern during the Medieval Climate Anomaly? PAGES newsletters 1, 16–18.
Moreno, A., Pérez, A., Frigola, J, Nieto-Moreno, V., Rodrigo-Gámiz, M., Martrat, B., González-Sampériz, P., Morellón, M, Martín-Puertas, C, Corella, J.P., Belmonte, A., Sancho, C., Cacho, I, Herrera, G., Canals, Grimalt, J., M, Jiménez-Espejo, F., Martínez-Ruiz, F., Vegas-Vilarrúbia, Valero-Garcés, B.L., 2012. The Medieval Climate Anomaly in the Iberian Peninsula reconstructed from marine and lake records. Quaternary Science Reviews 43, 16–32.
Mulder, T., Alexander, J., 2001. The physical character of subaqueous sedimentary density flows and their deposits. Sedimentology 48, 269–299.
Ninyerola, M., Pons, X., Roure, J.M., 2005. Atlas climático Digital de la Península Ibérica. Metodología y aplicaciones en bioclimatología y geobotánica. Universidad Autónoma de Barcelona, Bellaterra.
Padisak, J., Borics, G., Fehér, G., Grigorszky, I., Oldal, I., Schmidt, A., Zámbóné-Doma, Z., 2003. Dominant species, functional assemblages and frequency of equilibrium phases in late summer phytoplankton assemblages in Hungarian small shallow lakes. Hydrobiologia 502, 157–168.
Rico, M.T., 2004. Las paleocrecidas en la cuenca media del Rio Segre durante el Pleistoceno superior-Holoceno: registros morfosedimentarios y análisis hidrológico. University of Zaragoza, Zaragoza.
Riera, S., Wansard, G., Julia, R., 2004. 2000-Year environmental history of a karstic lake in the Mediterranean Pre-Pyrenees: the Estanya lakes (Spain). Catena 55, 293–324.
Romero-Viana, L., Julià, R., Camacho, A., Vicente, E., Miracle, M., 2008. Climate signal in varve thickness: Lake La Cruz (Spain), a case study. Journal of Paleolimnology 40, 703–714.
Rosell, J., 1994. Mapa Geológico de España y Memoria. Escala 1:50.000, Hoja de Tremp (252). Instituto Tecnológico Geominero de España (IGME), Madrid.
Rull, V., González-Sampériz, P., Corella, J.P., Morellón, M., Giralt, S., 2011. Vegetation changes in the southern Pyrenean flank during the last millennium in relation to climate and human activities: the Montcortès lacustrine record. Journal of Paleolimnology 46, 387–404.
Schaller, T., Wehrli, B., 1996. Geochemical-focusing of manganese in lake sediments—an indicator of deep-water oxygen conditions. Aquatic Geochemistry 2, 359–378.
Scussolini, P., Vegas-Vilarrúbia, T., Rull, V., Corella, J.P., Valero-Garcés, B.L., Gomà, J., 2011. Middle and late Holocene climate change and human impact inferred from diatoms, algae and aquatic macrophyte pollen in sediments from Lake Montcortès (NE Iberian Peninsula). Journal of Paleolimnology 46, 369–385.
Stabel, H.H., Chondrogianni, C., 1988. Seasonal shifts in the grain size of settling particles in Lake Constance. Water Research 22, 251–255.
Sturm, M., Matter, A., 1978. Turbidites and varves in Lake Brienz (Switzerland): deposition of clastic detritus by density currents. In: Matter, A., Tucker, M.E. (Eds.), Modern and Ancient Sediments. Blackwell, Oxford, pp. 147–168.
Thomas, J., Gonzalves, E.A., 1965. Thermal algae of western India III. Algae of the hot spring at Sav. Hydrobiologia 26, 1–316.
Tolotti, M., Corradini, F., Boscaini, A., Calliari, D., 2007. Weather-driven ecology of planktonic diatoms in Lake Tovel (Trentino, Italy). Hydrobiologia 578, 147–156.
Turney, C.S.M., Brown, H., 2007. Catastrophic early Holocene sea level rise, human migration and the Neolithic transition in Europe. Quaternary Science Reviews 26, 2036–2041.
Zhang, D.D., Brecke, P., Lee, H.F., He, Y.Q., Zhang, J., 2007. Global climate change, war, and population decline in recent human history. Proceedings of the National Academy of Sciences 104, 19214–19219.
Zolitschka, B., Behre, K.E., Schneider, J., 2003. Human and climatic impact on the environment as derived from colluvial, fluvial and lacustrine archives—examples from the Bronze Age to the Migration period, Germany. Quaternary Science Reviews 22, 81–100.

https://doi.org/10.1016/j.yqres.2012.06.002 Published online by Cambridge University Press